VOLUME 116, NUMBER 15
JULY 27, 1994

JOURNAL
OF THE
AMERICAN
CHEMICAL
SOCIETY

Inherent Conformation of the Biotin Bicyclic Moiety: Searching for a Role for Sulfur

George T. DeTitta,*,† Robert H. Blessing,† Grant R. Moss,‡ Harry F. King,§ Dinesh K. Sukumaran,§ and Raymond L. Roskwitalski§

Contribution from the Medical Foundation of Buffalo, Buffalo, New York 14203, and Department of Chemistry, State University of New York at Buffalo, Buffalo, New York 14214

Received June 28, 1993⊗

Abstract: The inherent conformation of the biotin bicyclic moiety has been examined. In biotin and various heterobiotins the *endo* conformation of the bicyclic ring is always observed; however, the presence of a side chain in the native coenzyme and its analogs may preclude the alternative *exo* conformation, masking what may be an inherently more favored conformation. The crystal structures of the three chainless analogs of biotin, oxybiotin, and azabiotin have been determined, and in all cases the bicyclic rings adopt the *endo* conformation, with the heteroatom proximal to the ureido ring. In contrast, *ab initio* quantum calculations and high-resolution nuclear magnetic resonance experiments on the chainless analog of biotin suggest that the *endo* and *exo* conformations of the bicyclic ring are of comparable energy and coexist in approximately equal amounts in solution.

Introduction

Biotin (**1**) is a coenzyme involved in carbon dioxide uptake, transfer, and removal reactions.[1] Structurally it is composed of a pentanoic acid side chain and a bicyclic moiety that contains sulfur.[2] The side chain is thought to act principally as a covalent linking agent that binds the bicyclic moiety, via an amide bond to the ε-amino group of a lysine residue, to the enzymes that biotin serves.[3] All of the chemistry catalyzed by the coenzyme is thought to take place on the ureido ring of the bicyclic moiety, or more specifically at the $N_{1'}$ nitrogen.[4] The role of sulfur in biotin-mediated biochemistry is a question of long standing.[5-15]

In the native coenzyme the bicyclic moiety adopts an *endo* conformation, Figure 1a, with the sulfur atom proximal to the ureido ring.[10] An alternative *exo* conformation, Figure 1b, with the sulfur atom distal to the ureido ring, is presumably precluded by a close contact between the side chain and the bicyclic moiety that would result. The question arises as to the inherently more

† Medical Foundation of Buffalo.
‡ Permanent address: BHP Petroleum, 120 Collins St., Melbourne, Australia.
§ State University of New York at Buffalo.
⊗ Abstract published in *Advance ACS Abstracts*, June 15, 1994.

(1) Moss, J.; Lane, M. D. In *Advances in Enzymology*; Meister, A., Ed.; Interscience Publishers: New York, 1971; pp 321–442.
(2) Melville, D. B.; Moyer, A. W.; Hofmann, K.; du Vigneaud, V. *J. Biol. Chem.* **1942**, *146*, 487–492.
(3) Kosow, D. P.; Lane, M. D. *Biochem. Biophys. Res. Commun.* **1962**, *7*, 439–443.
(4) Lynen, F.; Knappe, J.; Lorch, E.; Jütting, G.; Ringelmann, E. *Angew. Chem.* **1959**, *71*, 481–486.
(5) Lane, M. D.; Young, D. L.; Lynen, F. *J. Biol. Chem.* **1964**, 2858–2864.
(6) Glick, M. D.; Wormser, H. C.; Abramson, H. N. *Acta Crystallogr.* **1977**, *B33*, 1095–1101.
(7) Bowen, C. E.; Rauscher, E.; Ingraham, L. L. *Arch. Biochem. Biophys.* **1968**, *125*, 865–872.
(8) Sigel, H.; McCormick, D. B.; Griesser, R.; Prijs, B.; Wright, L. D. *Biochemistry* **1969**, *8*, 2687–2695.
(9) Mildvan, A. S.; Scrutton, M. C.; Utter, M. F. *J. Biol. Chem.* **1966**, *241*, 3488–3498.
(10) DeTitta, G. T.; Edmonds, J. W.; Stallings, W.; Donohue, J. *J. Am. Chem. Soc.* **1976**, *98*, 1920–1926.
(11) Chen, C.-S.; Parthasarathy, R.; DeTitta, G. T. *J. Am. Chem. Soc.* **1976**, *98*, 4983–4990.
(12) Sigel, H.; Scheller, K. H. *J. Inorg. Biochem.* **1982**, *16*, 297–310.
(13) Fry, D. C.; Fox, T. L.; Lane, M. D.; Mildvan, A. S. *J. Am. Chem. Soc.* **1985**, *107*, 7659–7665.
(14) DeTitta, G. T.; Parthasarathy, R.; Blessing, R. H.; Stallings, W. *Proc. Natl. Acad. Sci. U.S.A.* **1980**, *77*, 333–337.
(15) Berkessel, A.; Breslow, R. *Bioorg. Chem.* **1986**, *14*, 249–261.

0002-7863/94/1516-6485$04.50/0

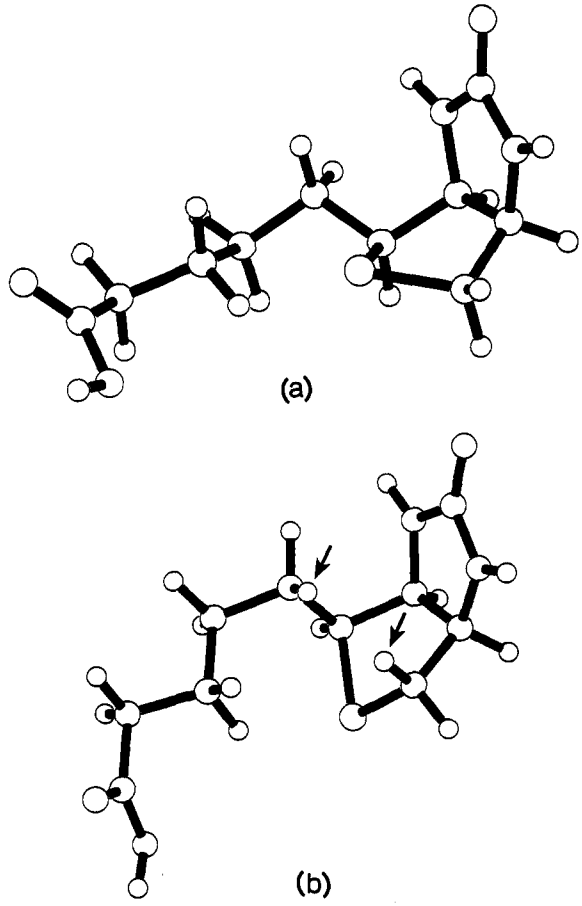

Figure 1. (a) Biotin in its native, *endo* conformation; (b) *exo*-biotin with the sulfur atom flapped down (the ureido group at the top of the figure defines the up direction) and the attendant $H_{5\beta'}\cdots H_6$ nonbonded contact of 2.05 Å (two hydrogen atoms indicated by arrows).

stable conformation of the biotin bicyclic moiety. Definite data favoring an *endo* conformation could be interpreted as evidence of a transannular interaction[9] stabilizing the more crowded conformer, whereas data favoring an *exo* conformation would be at odds with such an interpretation.

To address the issue we have studied the chainless analogs of biotin (**2**), oxybiotin (**3**), and azabiotin (**4**) by various techniques, including X-ray diffraction, high-resolution variable temperature nuclear magnetic resonance, and *ab initio* quantum chemical calculations. While only the *endo* conformer is observed in the crystalline state, the spectral and theoretical studies suggest a more complicated story.

Experimental Section and Results

Crystallography. Crystals of **2**, **3**, and **4** were grown from aqueous ethanol solutions. Suitable crystals for X-ray diffraction were screened by Weissenberg photography. Lattice parameters and intensity measurements were recorded on automatic diffractometers equipped with copper tubes that were nickel filtered. Intensity data were reduced to structure factors using routines written by one of us.[16] A summary of crystal data and experimental details is given in Table 1.

The crystal structure of **2** was determined by Patterson methods; those of **3** and **4** were determined by multisolution tangent formula methods. All three structures were refined to convergence by least-squares. The functions minimized were $\sum w_i(|F_i^{obs}|-|F_i^{calc}|)^2$ with weights $w_i = 1/\sigma_i^2$ where $\sigma_i \equiv \sigma(|F_i^{obs}|)$ includes contributions from counting statistics, background identification and subtraction, time-dependent scaling, and internal consistency. The results of the final cycles of refinement are summarized in Table 1, and the final positional parameters are given in Table 2. Hydrogen atom positions for the NH hydrogens were located in difference maps in all cases, including the secondary amine hydrogen atom in each of the molecules of **4**.

(16) Blessing, R. H. *Cryst. Rev.* **1987**, *1*, 3–58.

Table 1. Crystal and Experimental Data for X-ray Diffraction Studies of **2**, **3**, and **4**

	2	**3**	**4**
a (Å)	11.764(1)	15.525(2)	6.391(1)
b (Å)	5.550(1)	5.223(1)	10.719(2)
c (Å)	10.670(1)	15.556(3)	9.313(2)
β (deg)	111.66(1)	116.15(2)	104.18(2)
space group	$P2_1/C$	$P2_1/n$	$P2_1/c$
Z	4	8	4
formula	$C_5H_8O_1N_2S_1$	$C_5H_8O_2N_2$	$C_5H_9O_1N_3$
MW	144.20	128.13	127.15
ρ_c	1.479	1.503	1.365
$\mu(mm^{-1})_{Cu}$	3.693	0.950	0.788
standards	6	6	2
range (%)	12.9	0.5	13.2
N meas	1162	2505	1479
$I > 2\sigma I$	980	2188	945
h_{min}, h_{max}	−15, 15	−16, 15	0, 7
k_{min}, k_{max}	0, 8	0, 5	0, 13
l_{min}, l_{max}	0, 14	0, 16	−11, 11
$\sin\theta/\lambda_{max}$ (Å^{-1})	0.55	0.55	0.63
N_o	804	1476	1069
N_v	115	228	119
R	0.040	0.067	0.074
R_w	0.071	0.131	0.090
S	1.675	3.147	2.772

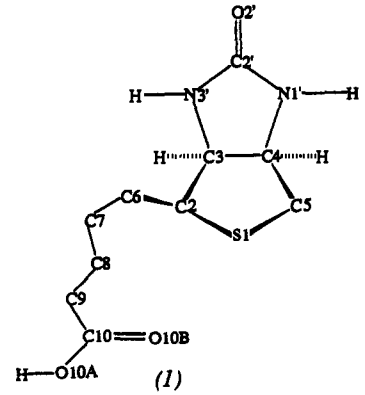

(1)

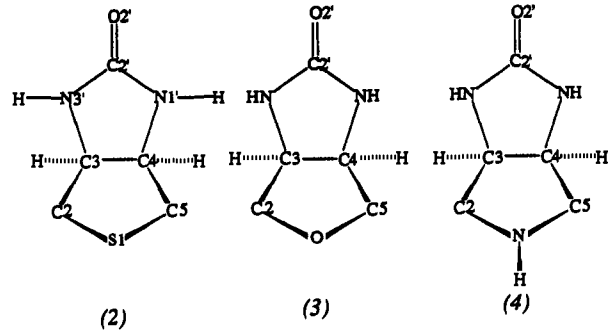

(2) (3) (4)

Crystals of **2** and **4** each contain one molecule in the asymmetric unit while crystals of **3** contain two independent molecules in the asymmetric unit. Thus there are four observations of the various heterobiotinyl bicyclic moieties where the *exo*-destabilizing contact has been eliminated. In all four instances the *endo* form is observed, Figure 2. In no instance is the *exo* form observed.

If we compare the molecular structures of **2**, **3**, and **4** with those of their respective intact analogs (**2** with biotin,[10] **3** with oxybiotin,[14] **4** with azabiotin[6]), it is evident that the absence of the pentanoic acid side chain allows the bicyclic rings of each of the chainless analogs to realize, to a much fuller extent, their

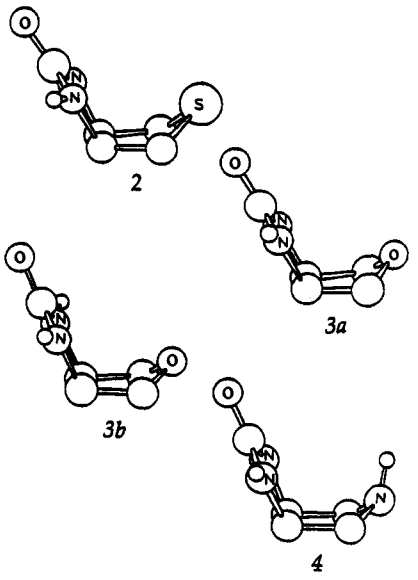

Figure 2. The crystallographically observed conformations of **2**, **3** (two independent molecules in the crystal chemical unit), and **4** drawn so as to emphasize the *endo* conformation of the bicyclic ring. Only NH hydrogen atoms are shown.

chemically present (but not crystallographically required) mirror symmetry. Thus the bicyclic ring asymmetry[10] parameters Φ_B are close to 0 for the chainless analogs, Table 3, but are larger for the native heterobiotins. This is especially true for **3** and **4** as compared to oxybiotin and azabiotin, respectively. Thus while oxybiotin and azabiotin are maximally distorted from mirror symmetry, their respective chainless analogs are not. Biotin itself is unique in that both the native coenzyme and its chainless analog assume nearly perfect mirror symmetry.

Out-of-plane distances of the heteroatoms (S, O, N) from the C_2–C_3–C_4–C_5 least-squares planes, Figure 3, are similar for the native and chainless structures. The sulfur atom in biotin[10] is 0.87 Å out of the plane; in **2** it is 0.84 Å. Bond distances and angles are comparable as well. The ureido ring bond distances, Figure 3, are indicative of a partially delocalized system,[17] with $C_{2'}$=$O_{2'}$ slightly longer than a typical C=O double bond and the carbonyl C—N bonds slightly shorter than typical C—N single bonds.

No two of the crystal packing motifs of **2**, **3**, and **4** are identical, Figure 4, but there are features common to all three. Each molecule forms a hydrogen-bonded ring of the type

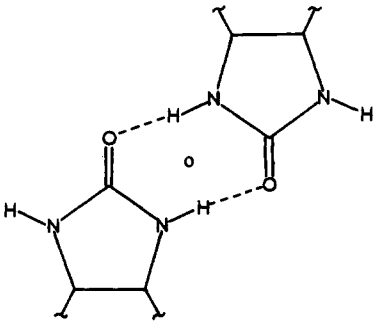

about a crystallographic center of symmetry. Similar rings are found[14] in the structures of biotin methyl ester, oxybiotin, and biotin-*d* oxide. The N···O distances are 2.90 ± 0.1 Å. In the crystal structure of **3** the ether oxygen atoms accept the remaining NH···O hydrogen bonds. Each crystallographically independent molecule in the structure of **3** hydrogen bonds only with symmetry mates of itself, forming two separate two-dimensional layers that are not hydrogen bonded to one another. In the crystal structure of **4** there is true three-dimensional hydrogen bonding. The secondary amine NH accepts a hydrogen bond from a neighboring ureido NH and in turn donates a hydrogen bond to a ureido oxygen atom. In both molecules of **4** the secondary amine hydrogen atom, located in difference maps, is in the *endo* position, pointing in toward the pockets of the molecules. Only in the crystal structure of **2** is the heteroatom absent from the hydrogen-bonding network. There, a second ureido NH···O hydrogen bond forms bilayers of **2** such that all of the hydrogen bonding lies buried in the interior of the bilayers while the tetrahydrothiophene rings protrude outward, forming the outer surfaces of, and interfaces between, bilayers.

Interaction Energy of the Crystal Structure of 2. The consistent observation of a preferred *endo* conformation in the diffraction analyses might be ascribed in some quarters to the effects of crystal packing forces. Since the heteroatoms (oxygen and nitrogen) substituting sulfur in molecules **3** and **4** are integrally a part of the hydrogen bonding of their respective crystal structures, such claims are as difficult to substantiate as to deny. However, in the crystal structure of **2** the sulfur atom plays no role in the hydrogen bonding and we might ask if the *exo* conformation of **2** is precluded by crystal packing considerations.

One approach to such a question is afforded by the atom–atom potential method[18] in which the interaction energy of a single molecule with its environment is calculated. Terms included in the calculation are those arising from electrostatic, dispersion, and repulsion energies but not polarization energies. A preliminary calculation on a fragment of the observed crystal structure of **2** was undertaken to give a base line for comparison. A bilayer composed of five unit cells along *c* and seven unit cells along *b*, or a total of $4 \times 5 \times 7 = 140$ molecules, was extracted directly from the crystal structure of **2**, Figure 5a. Hydrogen atoms were positioned at their ideal geometries using standard bond lengths, bond angles, and torsion angles. Using the formalism of Huron and Claverie[18] and parameters they estimate for hydrogen, carbon, nitrogen, and sulfur atoms, a calculation of the interaction energy of a single molecule in the center of the 140-molecule cluster with its 139 neighbors yields a base-line energy of -18.3 kJ·mol^{-1}. To test if a bilayer of similar dimensions (140 molecules) composed exclusively of the *exo* form of **2** is viable, a theoretical *exo* bilayer was constructed from the experimental *endo* bilayer by removal of the four methylene group hydrogens flanking the sulfur atoms, inversion of the positions of the sulfur atoms through the planes made by the carbon atoms of the thiophene rings from their *endo* to their *exo* positions, and addition of the four methylene group hydrogen atoms, once more at their idealized geometries, for each of the 140 molecules in the bilayer, Figure 5b. Again the interaction energy of the central molecule in the bilayer was calculated, this time as -17.5 kJ·mol^{-1}. It should be emphasized that there are no terms that represent intramolecular atom–atom energies in either sum, nor was either bilayer allowed to relax at all from its specified (experimental or generated) geometry. At the level of approximation of the theory we conclude that the *endo* and the *exo* bilayers are of comparable interaction energy.

To show that the *exo* form is not excluded by crystal packing effects, we undertook a second set of calculations. In this set, a second bilayer was constructed and allowed to slide over the first, allowing for translations in three orthogonal directions of one bilayer with respect to the other, Figure 6a. The three translations were designed to correspond to two that slide one bilayer over the other and one that controls the distance between bilayers. In view of the translational periodicity of the crystal lattice and the noncooperativity of the atom–atom approach, it is sufficient to model the second bilayer by a single molecule of **2** oriented as in its crystal structure. A benchmark calculation on the *endo* form was performed. The second bilayer, as represented by the single molecule, was allowed to translate rigidly (without rotation)

(17) Blessing, R. H. *J. Am. Chem. Soc.* **1983**, *105*, 2776–2783.

(18) Huron, M.-J.; Claverie, P. *J. Phys. Chem.* **1974**, *78*, 1862–1867.

Table 2. Positional Parameters for **2** (X = S), **3** (X = O), and **4** (X = N)

atom	parameter	2	3a	3b	4
X(1)	x	0.415 66(4)	0.342 82(8)	0.190 65(8)	0.474 79(36)
	y	0.155 31(11)	0.239 40(25)	0.279 01(28)	0.218 70(19)
	z	0.114 55(5)	−0.309 21(8)	0.348 44(9)	0.282 61(23)
C(2)	x	0.334 41(21)	0.444 65(11)	0.200 31(14)	0.477 25(40)
	y	0.155 30(44)	0.238 09(36)	0.022 32(46)	0.121 62(26)
	z	0.228 77(21)	−0.262 72(12)	0.319 05(14)	0.172 64(28)
C(3)	x	0.205 03(16)	0.472 44(11)	0.303 41(11)	0.264 98(39)
	y	0.070 96(38)	0.100 75(35)	−0.049 46(34)	0.047 76(23)
	z	0.145 94(17)	−0.168 23(12)	0.381 67(11)	0.152 01(25)
C(4)	x	0.208 33(16)	0.384 95(12)	0.331 77(12)	0.115 45(38)
	y	−0.098 09(35)	0.074 40(32)	0.114 34(36)	0.136 12(22)
	z	0.032 00(19)	−0.188 35(12)	0.473 84(12)	0.213 96(26)
C(5)	x	0.341 12(19)	0.316 19(12)	0.241 22(12)	0.247 67(45)
	y	−0.121 88(39)	−0.012 73(38)	0.270 54(38)	0.254 82(23)
	z	0.042 80(22)	−0.291 79(12)	0.450 58(13)	0.253 25(30)
N(1′)	x	0.133 45(15)	0.352 10(9)	0.411 15(10)	0.088 24(35)
	y	0.028 26(31)	0.012 33(32)	0.263 82(33)	0.068 71(19)
	z	−0.088 73(13)	−0.120 09(9)	0.476 55(10)	0.343 57(23)
C(2′)	x	0.083 00(17)	0.404 34(11)	0.431 45(10)	0.188 71(35)
	y	0.227 41(38)	0.208 77(34)	0.219 89(34)	−0.042 35(20)
	z	−0.062 11(17)	−0.065 96(10)	0.402 14(11)	0.360 71(26)
O(2′)	x	0.007 15(13)	0.389 64(8)	0.494 11(8)	0.191 31(28)
	y	0.359 12(25)	0.320 72(27)	0.327 07(29)	−0.118 44(15)
	z	−0.146 48(13)	−0.003 57(8)	0.386 83(8)	0.462 35(20)
N(3′)	x	0.127 39(14)	0.472 98(10)	0.370 38(10)	0.284 97(35)
	y	0.264 93(31)	0.265 48(32)	0.040 36(32)	−0.059 03(20)
	z	0.071 45(14)	−0.093 65(10)	0.345 58(9)	0.249 51(23)

Table 3. Asymmetry Parameters for **2**, **3a**, **3b**, and **4** from the Crystallographic Studies[a]

	Φ_U, deg	Φ_H, deg	Φ_B, deg
2	1.0	0.4	0.5
3a	2.7	1.8	2.5
3b	2.0	2.6	2.7
4	5.8	5.3	5.6

[a] The measures are as follows: Φ_U, the ureido ring ΔC_s asymmetry parameter; Φ_H, the heteroatom ring ΔC_s asymmetry parameter; Φ_B, the overall bicyclic ring ΔC_s asymmetry parameter. A large asymmetry parameter is a consequence of a large departure from C_s (mirror) symmetry.

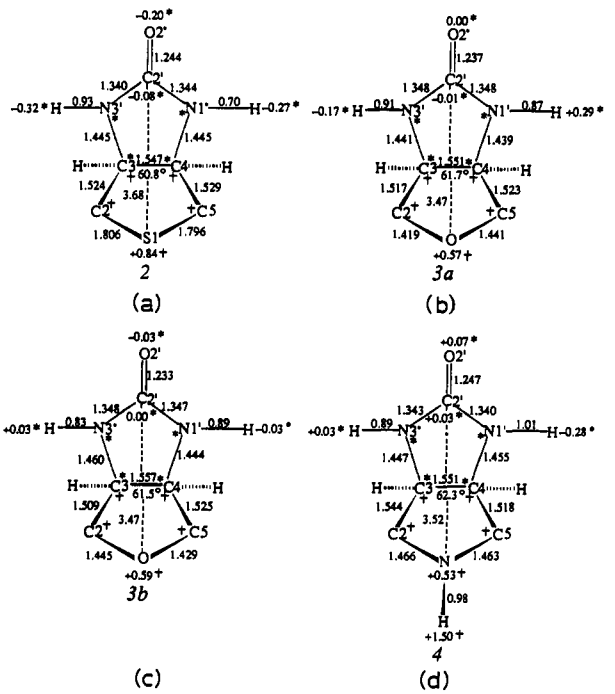

Figure 3. Crystallographically determined dimensions of the chainless vitamers **2**, **3** (two independent molecules), and **4**. Dimensions marked with asterisks and plus signs indicate distances from the least-squares planes fitted to $\{N_{3'}, C_3, C_4, N_{1'}\}$ (*) and $\{C_2, C_3, C_4, C_5\}$ (+). Positive directions are toward the viewer. The angle between the least-squares planes is given just below the C_3–C_4 bond. The $C_{2'}\cdots X$ nonbonded distances (X = S, O, N) is lettered in vertically.

with respect to the first bilayer, and a minimum in the interaction energy of −18.2 kJ·mol^{-1} was located. The position of the minimum allows the recalculation of the corresponding crystal structure lattice parameters. Only $|a|$ and β are affected by the rigid translation since b and c form the plane of the bilayer. By the requirement of simple rectilinear motions (no rotation of the second bilayer permitted), space group symmetry is preserved. The recalculated $|a|$ and β values, 11.62 Å and 110.5°, respectively, compare very well with the true crystal values, 11.64 Å and 110.8°, respectively. Thus the simple atom–atom approach predicts the bilayer–bilayer separation and translation that is observed in the *endo* crystal structure. A final calculation to test the postulated *exo* crystal structure was performed. The theoretical *exo* bilayer was probed by a second *exo* bilayer, as modeled by a single molecule of **2** in its *exo* form, Figure 6b. Again only rigid translations of one bilayer with respect to the other were allowed, and again the translations were arranged so that two represented movements parallel to the bilayer plane and one represented a bilayer–bilayer separation. The minimum of interaction energy, −16.3 kJ·mol^{-1}, is slightly higher than that for the observed *endo* form and corresponds to a crystal structure elongated along a to 12.72 Å and opened up about the interaxial angle β to 119.1°. The elongation is primarily due to the extension of the molecular length in going from the *endo* to the *exo* form.

***Ab Initio* Quantum Chemical Calculations.** A simple examination of molecular models does not suggest why an *endo* conformation for the chainless derivatives should be preferred over an *exo* conformation. Therefore we undertook a series of quantum chemical calculations to identify and quantify stationary points on the potential energy surface of **2**. Energy minimum geometries were located using the GRADSCF suite of programs.[19] Energy-optimized geometries were located by calculating analytic first derivatives of the total energy with respect to the nuclear positions. Preliminary calculations on the five-membered-ring subgroups of the bicyclic moiety suggested that while electron correlation effects could be important in determining the absolute

(19) GRADSCF is an *ab initio* gradient program system written and designed by A. Kormornicki at Polyatomics Research Institute.

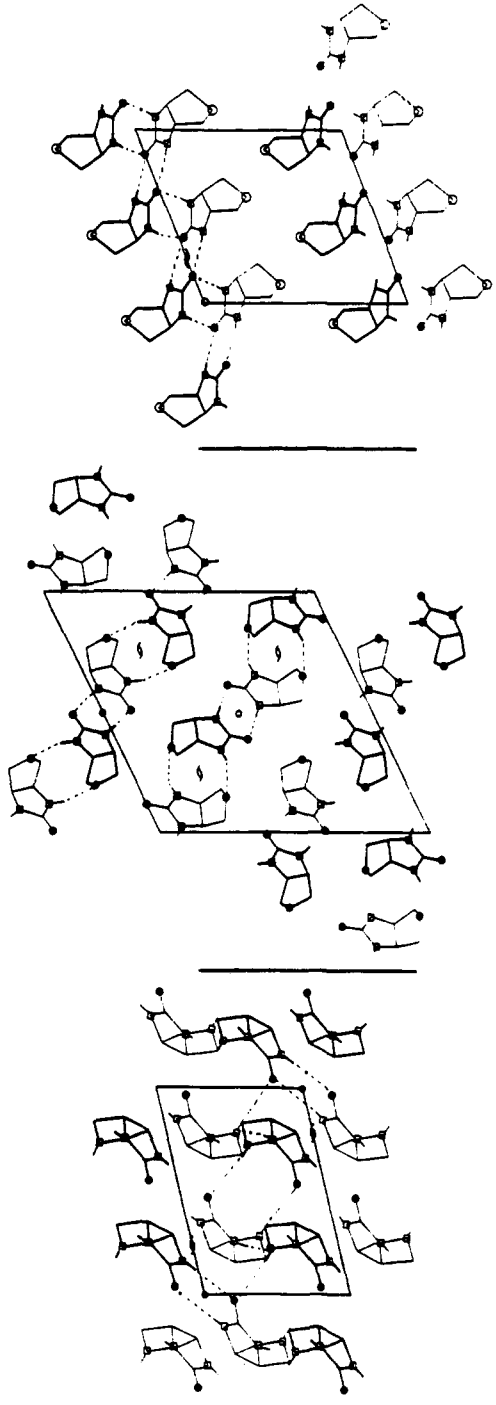

Figure 4. Crystal structures of **2**, **3**, and **4** (top to bottom). Views are projections on the *ac* planes, with origins at lower left, $+a$ horizontal, $+c$ just left of vertical, in all cases. Bilayers of **2** are coming out of the page, while bilayer–bilayer interactions are left–right. Molecules of **3** are segregated, those of each type hydrogen bonding only with symmetry mates of their own kind. Hydrogen bonding in **4** is three-dimensional.

total energy of a particular geometry, comparative analysis of two geometries did not require the incorporation of correlation into the calculation. Furthermore, the preliminary calculations, undertaken with a variety of basis set sizes, indicated that reliable ΔE values could be obtained at the 6-31G* level.

Although not required by the explicit imposition of symmetry in the calculations, all of the stationary points of the potential energy surface of **2** display bilateral mirror (C_s) symmetry. These points include geometries in which the ureido and tetrahydrothiophene rings of **2** are either flat, folded inward (*endo*), or folded outward (*exo*), Figure 7. The folded ureido rings fold about a line connecting the two nitrogen atoms while the folded

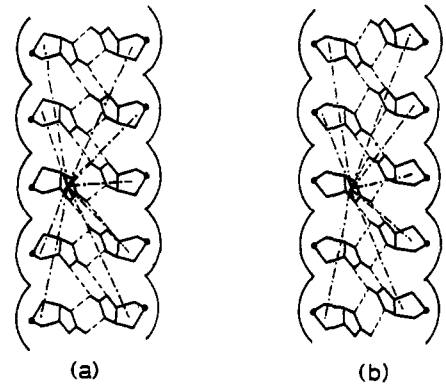

Figure 5. A fragment of the 140-molecule bilayer of **2** used in the atom–atom potential calculations. Light lines indicate hydrogen bonding that maintains the bilayer. Dashed lines are meant to indicate that the calculations include contributions from a central molecule to its 139 neighbors in the bilayer. Hydrogen atoms are not shown but are included in the calculations. (a) *Endo* conformation abstracted from crystal structure; (b) *exo* conformation generated from the *endo* conformation as described in the text.

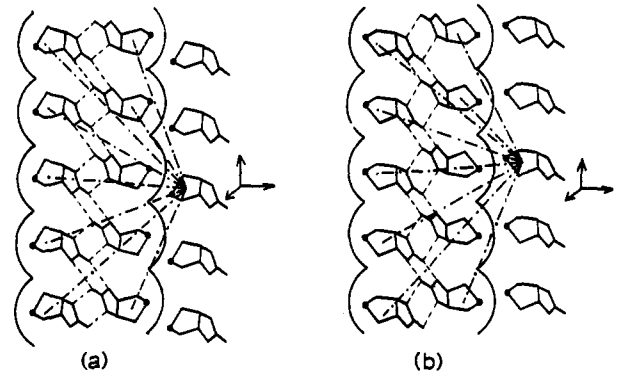

Figure 6. The 140-molecule bilayer probed by a second bilayer as represented by a single molecule. Light lines indicate hydrogen bonding that maintains the bilayers. Dashed lines are meant to indicate that the calculations include contributions from all 140 molecules of the bilayer on the left to the single molecule on the right. Shown are the energy minima calculated as the second bilayer is allowed to translate rigidly with respect to the first. (a) *Endo* bilayers with minimum at observed crystal structure; (b) *exo* bilayers.

tetrahydrothiophene rings fold about a line connecting the two methylene carbon atoms. Of the three-by-three combinations of ureido and tetrahydrothiophene ring geometries, Figure 7a–i, it proved possible to locate seven of the nine potential stationary points.

Stationary points corresponding to the two-by-two combinations of ureido ring folded in or out and the tetrahydrothiophene ring folded *endo* or *exo*, Figure 7a,c,g,i, were examined with a 6-31G* basis set. Geometry-optimized structures corresponding to true minima on the potential energy surface were located for three of the four combinations. It proved to be impossible to locate the stationary point corresponding to a structure with an *exo* tetrahydrothiophene ring and an inwardly folded ureido ring, Figure 7g. One of the minima, with an *endo* tetrahydrothiophene ring and an outwardly folded ureido ring, Figure 7c, corresponds closely to the structure observed in the crystalline state. It has a calculated energy 0.473 kJ·mol^{-1} higher than the global minimum, i.e., the structure with an *exo* tetrahydrothiophene ring and an outwardly flapped ureido ring, Figure 7a. The third stationary point we were able to locate corresponds to a structure with both rings folded inward, Figure 7i; its energy is 0.375 kJ·mol^{-1} above that for the global minimum.

Comparison of the geometry of the energy-minimized structure most closely resembling that found in the crystalline state, Figure 7c, with the diffraction results suggests that there is good

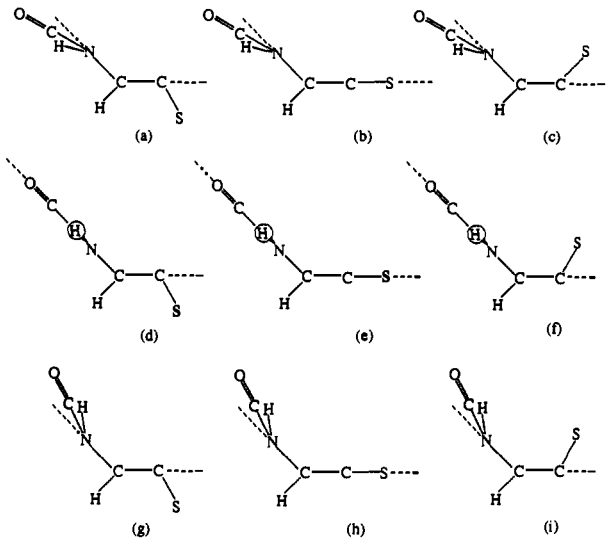

Figure 7. The nine stationary points on the STO-3G potential energy surface (PES) of **2**. Projections are along bridgehead bond C_3–C_4. Dashed lines are projections of the planes defined by $\{C_2, C_3, C_4, C_5\}$ (horizontal) and $\{N_{1'}, C_4, C_3, N_{3'}\}$ (off vertical). Distances from these planes are exaggerated for clarity. Structures b, e, and h are saddle points in the STO-3G PES; all the rest are minima. Structure c closely resembles the crystal structure of **2**; structure a is the minimum energy structure on the 6-31G* PES; structure g is a stationary point on the STO-3G PES, but not on the 6-31G* PES.

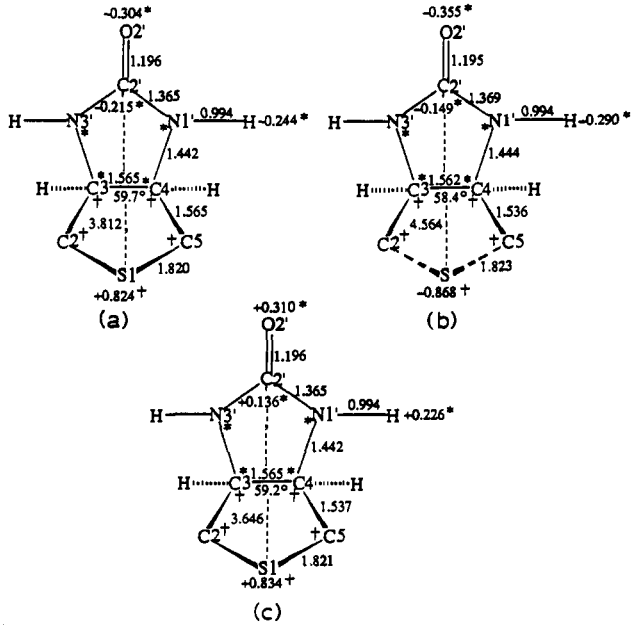

Figure 8. Dimensions of **2** from geometry optimization at the 6-31G* level. See the caption below Figure 3 for further details. (a) Conformation (Figure 7c) most closely resembling crystal structure results; (b) the global energy minimum (Figure 7a); (c) a minimum of energy between a and b.

agreement between the two. In both, the bond lengths between non-hydrogen atoms are in good correspondence, Figure 8a versus Figure 3a. The largest difference is for the $C_{2'}$=$O_{2'}$ bond in the ureido ring, which is larger in the crystalline state than calculated for the isolated molecule (1.244 Å vs 1.196 Å, respectively). To a lesser extent the $C_{2'}$–$N_{1'}$ and $C_{2'}$–$N_{3'}$ bonds in the crystalline state are concomitantly smaller than those for the isolated molecule (1.334 and 1.340 Å vs 1.365 Å). These small, systematic differences between results in the crystalline state and in the isolated molecule are real effects due to hydrogen bonding; they

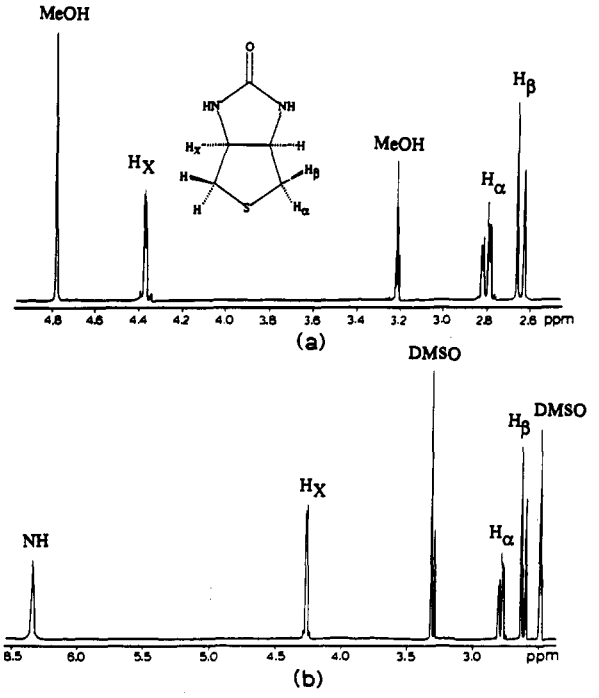

Figure 9. The 400-MHz proton spectrum of **2** in (a) deuteriomethanol and (b) deuterio-DMSO at 293 K. See text for proton assignments.

parallel results obtained for glycoluril,[20] an analog of **2**. In calculations performed on a fragment of the crystal structure of glycoluril, in which hydrogen bonding to the ureido oxygen atoms and from the ureido NH groups is modeled, the C=O bonds lengthen and C—N bonds shorten to agree much more closely with those observed in the crystalline state. The inverse relationship between the ureido C=O and C—N bond lengths, as well as its relevance to the various electronic states that are obtained in the urea chemical functionality, has been the subject of much study.[17]

High-Resolution Nuclear Magnetic Resonance.

While a clear preference for the *endo* form in the crystalline state is evident, quantum chemical calculations predict a number of conformers, both *endo* and *exo*, to be of comparable energy. We therefore undertook to investigate the solution properties of **2** by high-resolution NMR spectroscopy.

Spectra for **2** in deuteriomethanol and deuterio-DMSO were recorded at various temperatures between 293 and 333 K on a Varian 400S spectrometer operating at 399.98 MHz for ^{1}H. Sample concentrations were 5 mg·mL^{-1}. Solvents were from Cambridge Isotope Laboratories. Spectra were recorded with a digital resolution of better than 0.005 Hz/point and were Fourier transformed back into the frequency domain without the application of windowing functions. Typically 32 scans were accumulated for each spectrum with a 3-s delay for sample relaxation between scans. The spectra for **2** are shown in Figure 9; selected portions of the spectra at various temperatures are shown in Figure 10.

Proton assignments are in accord with those for norbiotin[21] and biotin.[22] The NH hydrogens are seen in the DMSO-d_6 spectrum at 6.3 ppm, the bridgehead hydrogens H_3 and H_4 at 4.3 ppm, the α hydrogens $H_{2\alpha}$ and $H_{5\alpha}$ at 2.8 ppm, and the β hydrogens $H_{2\beta}$ and $H_{5\beta}$ at 2.6 ppm. The coupling of the bridgehead hydrogens with the α and β hydrogens should be indicative of the form (or forms) of **2** in solution. In particular the ^3J coupling between $H_{2\beta}$ and H_3 (and by symmetry $H_{5\beta}$ and H_4) should be small or 0[23]

(20) Li, N.; Maluendes, S.; Blessing, R. H.; Dupuis, M.; Moss, G. R.; DeTitta, G. T. *J. Am. Chem. Soc.*, following paper in this issue.
(21) Bradbury, J. H.; Johnson, R. N. *J. Magn. Reson.* **1979**, *35*, 217–222.
(22) Ikura, M.; Hikichi, K. *Org. Magn. Reson.* **1982**, *20*, 266–273.
(23) Knowles, J. R. *Annu. Rev. Biochem.* **1989**, *58*, 195–221.

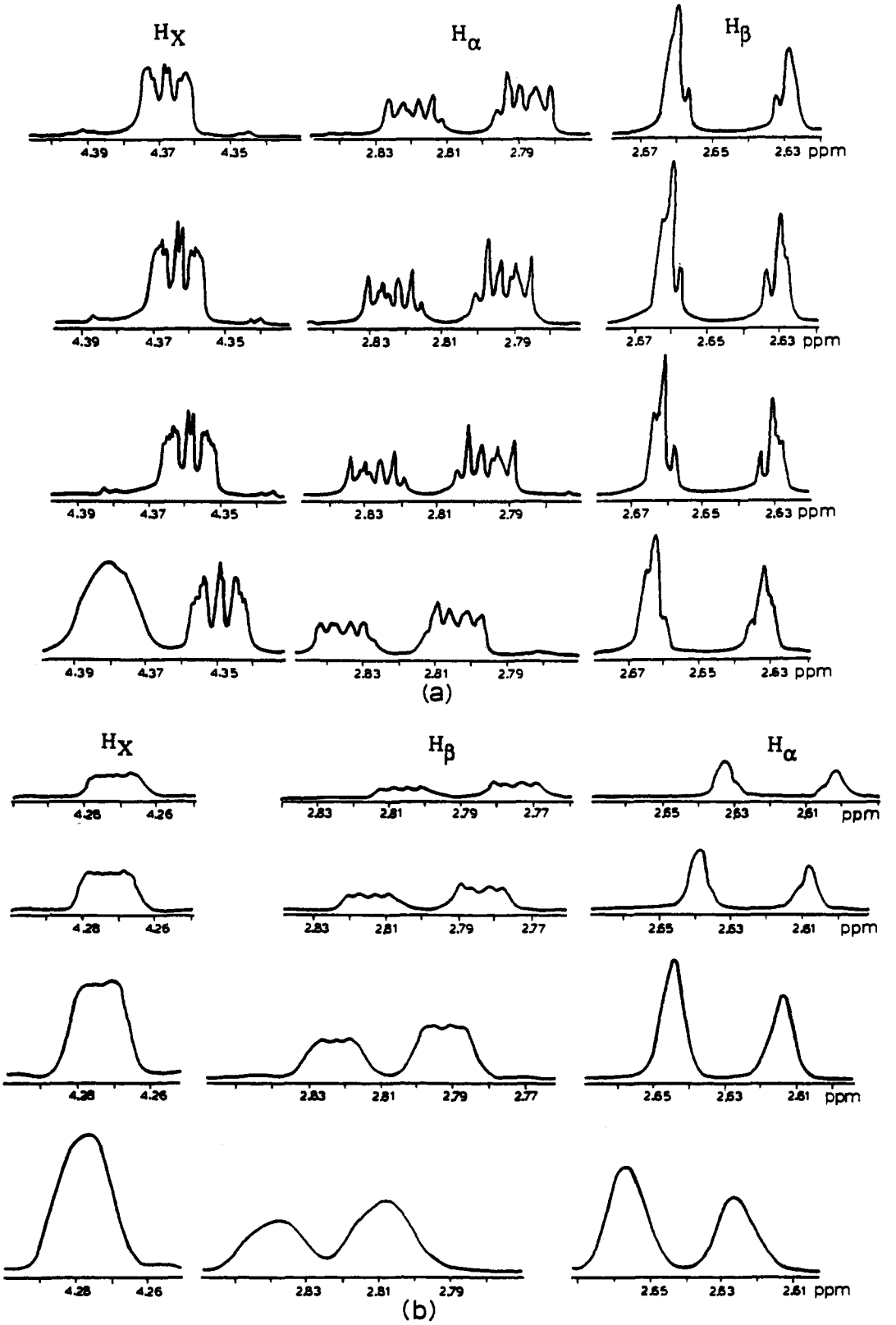

Figure 10. Selected portions of the NMR spectrum of **2**. Signals centered around 4.3 ppm are the bridgehead hydrogens H_3 and H_4, around 2.8 ppm are the α hydrogens $H_{2\alpha}$ and $H_{5\alpha}$, and around 2.6 ppm are the β hydrogens $H_{2\beta}$ and $H_{5\beta}$, (a) in deuterated methanol (CD_3OD) and (b) in deuterated DMSO [$(CD_3)_2SO_4$]. From top to bottom are spectra recorded at 293, 303, 313, and 333 K. The broad peak in the methanol spectrum at ~4.38 ppm recorded at 333 K is the methanol peak.

in the *endo* form because the torsion angles $H_{2\beta}$–C_2–C_3–H_3 and $H_{5\beta}$–C_5–C_4–H_4 are very close to 90° (89.7° from *ab initio* calculation of the geometry-optimized structure at the 6-31G* level).

Examination of the H_α region (~2.80 ppm) of the spectrum of **2** in methanol, Figure 10a, reveals a rich fine structure of as many as seven small peaks superimposed on each of the geminally split larger peaks. The H_β region (~2.65 ppm) reveals the presence of perhaps four small peaks superimposed on each of the geminally split larger peaks. The H_x region (~4.36 ppm) is also quite well developed, with a great deal of fine structure. As the temperature is raised from 293 K to 333 K there is a

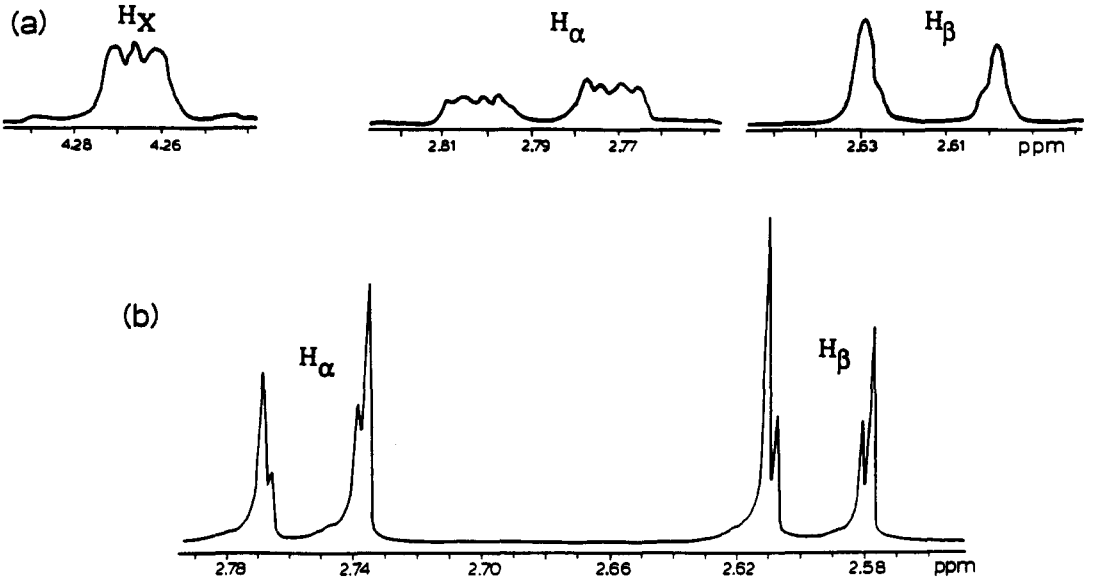

Figure 11. Double-resonance experiments on **2** at 293 K: (a) irradiating NH protons at 6.85 ppm in DMSO-*d*; (b) irradiating bridgehead protons H_3 and H_4 at 4.368 ppm in methanol-*d*.

gradual diminution in the sharpness of the spectral detail. This is more evident in an examination of the same features in DMSO, Figure 10b. There it is clear that, at 333 K, the spectra are very simple, only the $\alpha\beta$ geminal coupling surviving. The variations are reversible; fine structure is regained upon cooling. The reversible loss of fine structure upon warming suggests that two (or more) conformers of **2** are present in solution at 293 K and that, at that temperature, these conformers are interconverting slowly on the NMR time scale. A number of spectra were recorded under identical conditions of solvent and temperature at both 400 and 500 MHz; the spectra are invariant. Thus, the difference in the spectra of the conformers in solution is due to *J* coupling only.

A double-resonance experiment, Figure 11a, in DMSO in which the NH protons are irradiated shows that the richness of the spectra at the H_x, H_α and H_β positions is not due to coupling of the NH protons with the bridgehead protons H_x. Of course, the deuterated methanol spectra support that contention as well. But a double-resonance experiment, Figure 11b, in methanol in which the bridgehead protons H_x are irradiated clearly simplifies the H_α and H_β portions of the spectrum greatly. All that are left are two sets of geminally coupled peaks, of unequal magnitude.

The NMR results are in accord with the following interpretation. Both *endo* and *exo* conformers of **2** are present, and in slow equilibrium, at 293 K in methanol and DMSO. Double resonance at the bridgehead hydrogens (~4.3 ppm) leaves only the geminal coupling $^2J_{H_{2\alpha},H_{2\beta}} = {}^2J_{H_{5\alpha},H_{5\beta}}$. Apparently $^2J^{endo} \neq {}^2J^{exo}$, and therefore, two sets of doublets are present. The richness of the single-resonance spectra in the H_α and H_β positions is due to long-range (four bond) coupling $^4J_{H_3,H_{5\alpha}} = {}^4J_{H_4,H_{2\alpha}}$ and $^4J_{H_3,H_{5\beta}} = {}^4J_{H_4,H_{2\beta}}$. It is difficult to determine which of the two conformers predominates in solution, but we can argue that the H_β portion of the spectrum is more in line with a predominance of *endo* over *exo*; if it were the reverse, that portion would appear to be more clearly a doublet of a doublet, as the geminal coupling by H_α would be further split by a strong ^3J coupling of H_x and H_α (calculated torsion angles H_4–C_4–C_5–$H_{5\alpha}$ = H_3–C_3–C_2–$H_{2\alpha}$ = ±150.8° from *ab inito* 6-31G* geometry for the tetrahydrothiophene: *exo* form).

Discussion

The presence of sulfur in biotin constitutes a puzzle for those interested in the reaction chemistry of this coenzyme. Knowles[23] has recently reviewed the chemistry of biotin-dependent enzymes and has concluded his excellent account with a section entitled "Why Biotin?" Echoing that question has been the one, Why sulfur? Incorporation of sulfur into biotin comes late in its biosynthesis;[24] dethiobiotin is a precursor of biotin. If sulfur plays no role in the functioning of the vitamin, then the inactivity of dethiobiotin[1] as a coenzyme is not easily explained. Chemists have tended to look to a catalytic role for sulfur as an answer.

One such answer was that a transannular sulfur–carbonyl carbon interaction[9] might polarize the ureido carbonyl bond of $N_{1'}$-carboxybiotinyl-enzyme, thus facilitating a cyclic, concerted abstraction of hydrogen from pyruvate and insertion of CO_2. It has been subsequently demonstrated that the reaction is stepwise and not concerted.[25] Furthermore, it has been shown,[7] via infrared and NMR spectral studies, and through calculation of the overlap integrals for the S···$C_{2'}$ "bond" of biotin as a function of S–C separation, that a transannular effect is either exceedingly small or completely absent.[26] Nonetheless, the attractiveness of such an interaction, were it to exist, has prompted further study of the effect. Proton NMR studies of the exchange rate for the N_1·H hydrogen of biotin[13] suggested that a transannular effect was responsible for an apparently second order dependence of exchange on [H^+], but a reinvestigation[27] of that system has shown that the exchange is truly first order. In addition, investigations of the structure and spectral properties of adducts of biotin with various electrophiles[15] suggest that there is no evidence for a transannular effect. Among the evidence presented is the structure of the BF_3 adduct of biotin methyl ester in the crystalline state for which a S···C contact of 3.65 Å, not much smaller than that in biotin (3.68 Å), is observed. In addition, infrared and NMR spectral results on the adducts have been interpreted as incompatible with a transannular interaction.

Our results indicate a clear preference in the crystalline state for the *endo* conformation for chainless biotins. Of the four observations all are in the *endo* conformation, the conformation that minimizes the S···$C_{2'}$ nonbonded separation. The *exo* conformation for the intact coenzyme is not observed either in the crystalline state[10] or in solution. It was originally postulated[10] that the *exo* conformation was precluded by a close C_6···$N_{3'}$ contact that would result if the *endo* form shifted to the *exo*. In all likelihood a more compelling obstacle to inversion to an *exo* form is a resultant H···H nonbonded contact, 2.05 Å, between $H_{5\beta}$ and

(24) Eisenberg, M. *Adv. Enzymol.* **1973**, *38*, 317–372.
(25) O'Keefe, S.; Knowles, J. R. *J. Am. Chem. Soc.* **1986**, *108*, 328–329.
(26) Maggiora, G. M. *J. Theor. Biol.* **1973**, *41*, 523–534.
(27) Lett, R.; Marquet, A. *Tetrahedron* **1974**, *30*, 3365–3377.

one of the methylene hydrogens on C_6 of the side chain, Figure 1. But in **2** the *exo* form is excluded neither by a side chain nor by crystal packing considerations, as evidenced by our atom–atom calculations.

Our high-resolution proton NMR results are consistent with the existence of an equilibrium mixture of the *endo* and *exo* forms of **2** in solution, interconverting slowly on the NMR time scale at room temperature. We suggest that the *endo* conformer is in excess over the *exo*. Earlier studies of various derivatives of chainless biotins had been interpreted, on the basis of the coupling pattern between H_3 and $H_{2\beta}$ (and H_4 and $H_{5\beta}$), as showing exclusively the *endo* conformation in solution.[27,28] Our higher resolution studies show that this interpretation should be revised.

Our quantum chemical calculations fail to exhibit any supportive evidence for a transannular effect. Thus, in the progression of minimal energy structures from Figure 7a to Figure 7i to Figure 7c, the S···$C_{2'}$ nonbonded contact drops from 4.564 Å to 3.812 Å to 3.646 Å, respectively, yet the dimensions of the ureido ring, most notably the C═O and (O═)C—N bond distances, change very little, Figure 8. Our calculations on isolated molecules generally agree with the NMR results. The energy difference between the *endo* and *exo* forms is calculated to be very small in the extended basis set results, with a slight favoring of *exo* over *endo*, and the NMR results are interpreted as indicating a slight excess of *endo* over *exo* in solution. The basic conclusion to be drawn is that the two forms are of comparable energy.

The observation of the *endo* conformation exclusively in the crystalline state and its predominance in solution can be interpreted variously. First is the possibility that the *endo* form is inherently stabilized by some attractive feature, such as a transannular effect. To that we can counter that replacement of S by O or NH does not tip the balance, so if there is an attractive feature of the *endo* form it may not necessarily depend on the presence of sulfur. Second is the possibility that there is some inherently unattractive feature of the *exo* form. We have only quantum chemical data for the *exo* conformer; they do not suggest anything about this form that is energetically unattractive.

The sulfur of biotin is, if not absolutely essential for its catalytic role, at least highly desirable.[29] If we discount the transannular effect, we rule out an autocatalytic role for sulfur; whatever its role, it is not to activate the ureido portion of the coenzyme for its chemistry. This, however, does not rule out a catalytic function for sulfur entirely, for sulfur may be important in stabilizing the transition state of the other reactant in carboxylation reactions, namely, some form of bicarbonate. Current thinking[23] is that the ultimate reactants in the $N_{1'}$ carboxylation of biotinyl-enzyme are molecular CO_2 and the ureide anion of biotin. The CO_2 is thought to be generated *in situ* in an ATP-dependent dehydration reaction during which an unstable intermediate, carboxyphosphate, is formed. The intermediate decomposes to CO_2 and orthophosphate trianion, and the latter abstracts the N_1H hydrogen of biotin to form the ureide anion. These species may be reactive enough to account for the enzyme catalysis, but if a role for sulfur be necessary we can possibly find it in the interaction of the nucleophilic sulfur with the electrophilic carbon of CO_2. Such an interaction might tend to steer the reaction into the pocket formed by the two rings of biotin, as opposed to attack from the less hindered back side of the ureido ring.

Finally, it has to be admitted that sulfur may play no catalytic role whatever in biotion-mediated biochemistry. We have previously argued[11,14,19] that the sulfur of biotin may be geometrically required to secure a high degree of bilateral symmetry in the bicyclic ring, keeping the ureido group planar and therefore maximally conjugated. It is also likely that the precise positioning of the ureido group at the enzymatic catalytic sites is a consequence of the geometry at the bicyclic ring–pentanoic acid side chain junction, and we have already demonstrated[14] that that geometry is affected by the nature (and mere presence) of the heteroatomic species at the natural sulfur site. In the end, it may be sulfur simply because it fits.

Acknowledgment. This work was supported by Grants DK19856 and GM34073 from the National Institutes of Health and CHE-918022 from the National Science Foundation. We thank Professor Henry Wormser for the sample of chainless azabiotin and Professor Andrée Marquet for the samples of chainless biotin and chainless oxybiotin employed in the crystallographic studies. We also thank Dr. Mary McCourt, who offered valuable advice concerning the modeling of *exo*-biotin, and Dr. Andrew Kormornicki for the use of, and advice to one of us (H.F.K.) on the use of, GRADSCF.

(28) Bates, H. A.; Rosenblum, S. B. *Tetrahedron* **1985**, *41*, 2331–2336.

(29) Tipton, P. A.; Cleland, W. W. *J. Am. Chem. Soc.* **1988**, *110*, 5866–5869.